Cancer Imaging

CrossMark

Detection of gastric cancer and its histological type based on iodine concentration in spectral CT

Rui Li[1], Jing Li[2], Xiaopeng Wang[1], Pan Liang[1] and Jianbo Gao[1*]

Abstract

Background: Computed tomography (CT) imaging is the most common imaging modality for the diagnosis and staging of gastric cancer. The aim of this study is was to prospectively explore the ability of quantitative spectral CT parameters in the detection of gastric cancer and its histologic types.

Methods: A total of 87 gastric adenocarcinoma (43 poorly and 44 well-differentiated) patients and 36 patients with benign gastric wall lesions (25 inflammation and 11 normal), who underwent dual-phase enhanced spectral CT examination, were retrospectively enrolled in this study. Iodine concentration (IC) and normalized iodine concentration (nIC) during arterial phase (AP) and portal venous phase (PP) were measured thrice in each patient by two blinded radiologists. Moreover, intraclass correlation coefficient (ICC) was used to assess the interobserver reproducibility. Differences of IC and nIC values between gastric cancer and benign lesion groups were compared using Mann-Whitney U test. Furthermore, the gender, age, location, thickness and histological types of gastric adenocarcinoma were analyzed by Mann-Whitney U test or Kruskal-Wallis H test. Receiver operating characteristic (ROC) curves were used to evaluate the diagnostic efficacy of IC and nIC values, and the optimal cut-off value was calculated with Youden J.

Results: An excellent interobserver agreement (ICC > 0.6) was achieved for IC. Notably, the values of ICAP, ICPP, nICAP and nICPP were significantly higher in gastric cancer group ($Z = 5.870$, 3.894, 2.009 and 10.137, respectively; $P < 0.05$) than those in benign lesion group. Additionally, the values of ICAP, ICPP, nICAP and nICPP were significantly higher in poorly differentiated gastric adenocarcinoma group ($Z = 4.118$, 5.637, 6.729 and 2.950, respectively; $P < 0.005$) than those in well-differentiated gastric adenocarcinoma group. There were no statistically significant differences in the values of ICAP, ICPP, nICAP and nICPP between age, gender, tumor thickness and tumor location. Furthermore, the area under the curve (AUC) values of ICAP, nICAP, ICPP and nICPP were 0.745, 0.584, 0.662, and 0.932, respectively, for gastric cancer detection; while 0.756, 0.919, 0.851 and 0.684, respectively, in discriminating poorly differentiated gastric adenocarcinoma.

Conclusion: IC values exhibited great potential in the preoperative and non-invasive diagnosis of gastric cancer and its histological types. In particular, nICPP is more effective for the identification of gastric cancer, whereas nICAP is more effective in discriminating poorly differentiated gastric adenocarcinoma.

Keywords: Gastric, Adenocarcinoma, Spectral CT imaging, Iodine concentration, Histological degree

* Correspondence: gaojianbo_cancer@163.com
[1]Department of Radiology, the First Affiliated Hospital of Zhengzhou University, No. 1, East Jianshe Road, Zhengzhou 450052, Henan, China
Full list of author information is available at the end of the article

BMC

Li *et al. Cancer Imaging*   (2018) 18:42

Page 2 of 10

Background

Gastric cancer is the fifth most common cancer and the third leading cause of cancer-related deaths worldwide [1]. Gastric adenocarcinoma comprises 95% of all gastric cancers [2]. The incidence and mortality rates associated with gastric adenocarcinoma are both the highest among all malignant tumors of the digestive tract in China [3, 4], representing an emerging threat to human health. The mean survival time of patients with advanced gastric cancer is less than 1 year [5]. Therefore, early detection, diagnosis and treatment are advocated to improve the clinical outcomes and quality of life in patients with gastric cancer.

Histological grading has been considered a predictor of lymph node metastasis and poor survival in gastric cancer [6]. Hence, accurate assessment of histological types is crucial for individualizing patient management [7]. Gold standard for the diagnosis of gastric cancer and its histological types can be obtained through preoperative endoscopic biopsy in clinical practice. However, endoscopic biopsy is an invasive procedure, and may posses unavoidable sampling bias and incoincident with histological diagnosis during surgery [8]. As compared to invasive endoscopic biopsy, preoperative imaging technique offers many advantages as its non-invasive detection and histologic evaluation of tumors, as well as the assessment of regional or distant lymph node metastasis. Conventional contrast-enhanced CT imaging is the first-line imaging modality for the detection and staging of gastric cancer. Its combination with multiple planar reconstruction and virtual endoscopy has proven to be effective for the diagnosis of gastric wall invasion in patients with gastric cancer [9]. However, this technique relies solely on the morphological criteria, and lack of parameters for quantitative analysis.

Spectral CT provides material decomposition (MD) images that can quantitatively map the iodine concentration (IC) in the enhanced images of tissues. This IC value has been found to be strongly correlated with the actual IC in the phantom [10]. Preliminary studies have reported the use of IC value in differentiating benign from malignant lesions, evaluating tumor, node, and metastasis (TNM) staging and determining the efficacy of anticancer therapy [11–16]. However, to the best of our knowledge, only a few studies have employed IC value in discriminating the histological types of gastric adenocarcinoma [12, 17], and the results are inconsistent with respect to arterial phase (AP) and portal venous phase (PP). Indeed, the application of IC values for the discrimination of gastric cancer and its histological types is still in the exploratory stage.

Therefore, this study aimed to evaluate the diagnostic efficacy of IC values for the detection of gastric cancer and its histological type, and to investigate their correlations with clinical data.

Methods

Patients

Ethical approval was obtained from the institutional ethics review board, but the requirement of informed consent was waived due to the retrospective nature of the study. A total of 153 patients with gastric cancer and 45 patients with preoperative endoscopic biopsy-diagnosed benign gastric wall lesions (30 gastric inflammation and 15 normal gastric wall) who underwent spectral CT scans and surgical intervention were retrospectively enrolled from June 2013 to June 2016. Considering that the conditions of gastric wall beyond the sampling site are not accessible, the patients with gastric inflammation and normal gastric wall were grouped together. The exclusion criteria included pathologically-confirmed non-adenocarcinomas, history of preoperative therapy (such as radiotherapy and chemotherapy), severe artifacts on CT images, non-measurable lesions and incomplete clinical data. All the included patients completed the entire CT exam, and their gastric cavities were well distended on cross-sectional CT images without artifacts, and the gastric adenocarcinomas were clearly distinguished from normal gastric wall. Clinical data of patients, such as age, gender tumor thickness, tumor location and tumor differentiation were also documented.

CT scan protocol

After fasting for 8 h, patients were asked to consume 1000 mL of warm water and then injected with 20 mg of scopolamine (Specifications: 10 mg/mL; Hangzhou Minsheng Pharmaceutical Group Co., Ltd. Hangzhou, China) 10 min prior to examination. Patients were placed in the supine position, and scanned on GE Discovery CT750 HD scanner (GE Healthcare, Milwaukee, WI, USA) with gemstone spectral imaging (GSI) mode. Dual-energy CT images were acquired using a single x-ray source switches rapidly between 80 kVp and 140 kVp at less than 5 millisecond speed. The other acquisition parameters were as follows: 5 mm slice thickness, 40 mm detector coverage, 0.984 helical pitch, 630 mA tube current, 0.6 s rotation time, 512×512 matrix, and 40×40 cm field of view. AP and PP contrast-enhanced CT scans were performed with 40 and 70 s delays, respectively, after intravenous injection of 85–110 mL (1.5 mL per kg of body weight) iodinated contrast material (Ultravist 370, Bayer Schering Pharma, Berlin, Germany) at a rate of 3.0 ml/s through pump injector (Ulrich REF XD 2060-Touch, Ulrich Medical, Ulm, Germany). Contrast-enhanced CT images were reconstructed by using a standard kernel and 2.5 mm section thickness. The value of CT dose index volume (CTDIvol) for dual energy spectral mode in the abdomen was 23.84 mGy.

Image analysis

All data were transferred to GE AW 4.6 workstation (GE Healthcare, Milwaukee, WI, USA), and interpreted

Li *et al. Cancer Imaging* (2018) 18:42

Page 3 of 10

by two radiologists with 6 and 10 years of experience in gastrointestinal radiology. Data analysis was carried out independently using GSI Viewer software (GE Health-care, Milwaukee, WI, USA) with a standard soft-tissue window (WL 40 and WW 400). Regions of interest (ROI) were drawn on the solid part of the tumor (about two-thirds of the area), with the exclusion of peripheral fat, visible vessel, calcification and cystic/necrotic areas. A circular ROI was placed into the aortic arch within the same CT slice, after the exclusion of calcified athero-sclerotic plaque. Subsequently, the thickness of tumour was measured and recorded. In order to reduce the individual variation between patients, IC value was normalized by dividing the IC of lesion to that of aorta (nIC=IClesion/ICaorta) [12]. All IC values were repeatedly measured three times, and the average value was then calculated. Similarly, ROI of the three gastric regions (fundus, body and antrum) was measured for three times, and their average values were calculated.

Statistical analysis

All statistical analyses were performed with MedCalc v.9.2.0.0 (Frank Schoonjans, Broekstraat 52,B-9030 Maria-kerke, Belgium). P values of less than 0.05 were considered statistically significant. Interobserver agreement for IC and nIC values was evaluated using intraclass correlation coefficient (ICC), which classified as poor (< 0.40), fair (0.40–0.59), good (0.60–0.74), or excellent (0.75–1.00). The values of IC and nIC at both AP and PP were expressed as median (P25, P75). Mann-Whitney U test was used to compare the IC values between cancer and benign gastric wall group, as well as the IC values among age, gender, tumor thickness and histological types. Kruskal-Wallis H test was used to compare the differences of IC and nIC values between different tumour sites, including funtus, body and antrum. Furthermore, ROC curves were used to evaluate the diagnostic values of IC and nIC in discriminating gastric cancer and its histological type.

Results

Clinical data

A total of 87 (57%) out of 153 gastric cancer patients and 36 (80%) out of 45 patients with benign gastric wall lesions were ultimately included in the study. Among the excluded patients, 18 of them were diagnosed as non-adenocarcinoma by surgical pathology, 12 patients with poor image quality (severe artifacts) evaluated by two radiologists in consensus, and 8 patients received preoperative therapy. A further 9 patients with benign gastric wall lesions and 28 gastric cancer patients were excluded from analysis due to the non-measurable lesions on enhanced CT images. Overall, clinical data of 87 gastric adenocarcinoma patients and 36 patients with

benign gastric wall lesions were used for final analyses. The clinical characteristics of all included patients are summarized in Table 1, while the images of gastric adenocarcinoma patients at different sites are shown in Fig. 1.

Interobserver agreement

The interobserver agreement of IC measurement between two readers was ranked from good to excellent. In particular, the values of ICAP, ICPP, nICAP and nICPP in were 0.664, 0.755, 0.913 and 0.980, respectively, in gastric cancer group and 0.694, 0.713, 0.897, 0.910, respectively, in benign gastric wall lesions group. The mean difference between the two observers was used for further analysis.

Comparison of IC and nIC values between benign gastric wall lesions and gastric cancer

As shown in Fig. 2 and Table 2, the values of ICAP, ICPP, nICAP and nICPP in benign gastric wall lesions group were 9.388 (7.497, 12.740) 100 μg/ml, 17.233 (14.448, 18.798) 100 μg/ml, 0.111 (0.076, 0.141) and 0.264 (0.068, 0.328), respectively. On the other hand, the values of ICAP, ICPP, nICAP and nICPP in gastric cancer group were 12.900 (11.508, 14.832) 100 μg/ml, 20.000 (18.623, 22.000) 100 μg/ml, 0.115 (0.105, 0.141)

Table 1 Clinical characteristics of 87 patients with gastric adenocarcinomas and 36 patients with benign gastric wall lesions

Characteristics	Statistics(mean, range)
Cancer peoples	87
Age (years)	55 (29–74)
Gender(M/F)	60/27
Tumor thickness (cm)	3.1 (1.0–8.9)
Tumor site	
Fundus	29 (33.3%)
Body	28 (32.3%)
Antrum	27 (31%)
Whole stomach	3 (3.4%)
Histological differentiation degree	
Highly differentiated adenocarcinoma	4 (4.6%)
Moderately differentiated adenocarcinoma	40 (46.0%)
Poorly differentiated adenocarcinoma	43 (49.4%)
Benign lesion peoples	36
Age (years)	53 (32–72)
Gender(M/F)	22/14
Gastric wall	
Inflammation	25(69%)
Normal	11(31%)

Abbreviations:*M* Male, *F* Female
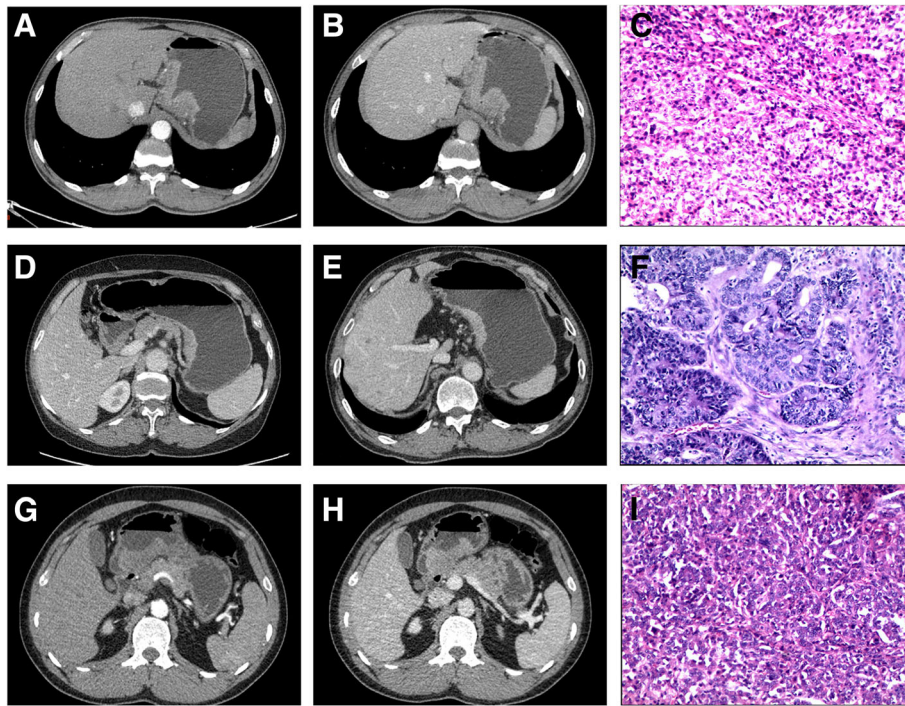
Fig. 1 Spectral CT images of patients with poorly and moderately differentiated gastric adenocarcinomas at different sites. **a** AP image shows moderate enhancement of fundal wall thickening in a 67-year-old male patient. The maximum thickness is 17.89 mm, and ICAP is 16.78 (100 μg/ml). **b** PP image demonstrates a ICPP value of 27.19 (100 μg/ml) in the same patient. c Photomicrograph of histological specimen indicates a poorly differentiated adenocarcinoma [hematoxylin and eosin (H&E) stain; original magnification × 100]. **d** AP image shows irregular wall thickening of the gastric body in a 41-year-old female patient. The maximum thickness is 14.24 mm, and ICAP is 14.46 (100 μg/ml). **e** PP image demonstrates a ICPP value of 24.57 (100 μg/ml) in the same patient. **f** Photomicrograph of histological specimen indicates a poorly differentiated adenocarcinoma. (H&E stain; original magnification × 100). **g** AP image shows antrum wall thickening with surface ulcers in a 56-year-old male patient. The maximum thickness is 20.32 mm and ICAP is 11.79 (100 μg/ml). **h** PP image demonstrates a ICP*P* value of 20.19 (100 μg/ml) in the same patient. **i** Photomicrograph of histological specimen indicates a moderately differentiated adenocarcinoma (H&E stain; original magnification × 100)
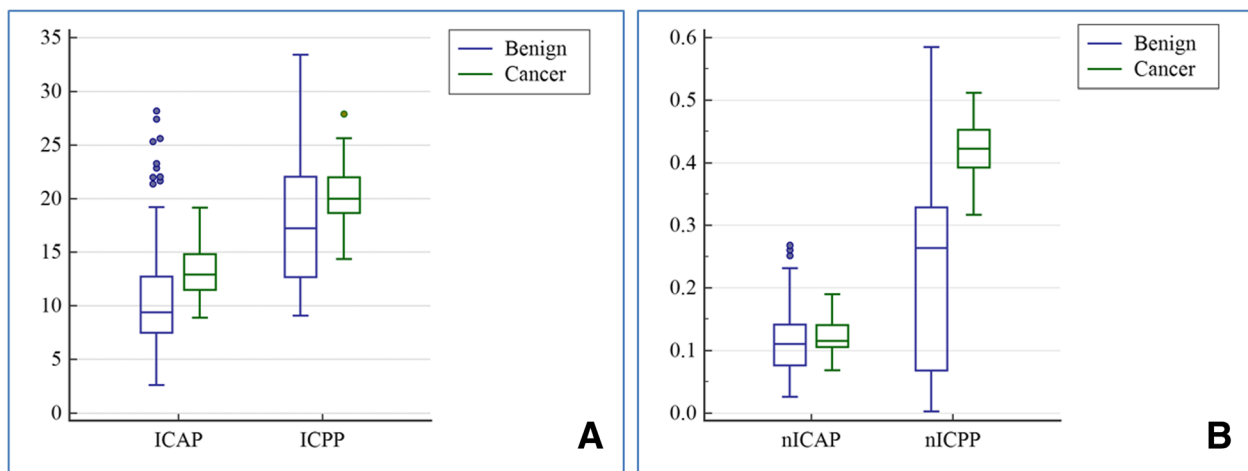
Fig. 2 Differences in IC and nIC values between between gastric cancer and benign lesion groups. Box-and-whisker plots (box: 25, 75%; centreline: medium; whisker: min, max) reveal that (**a**) ICAP, ICPP, (**b**) nICAP and nICPP of gastric adenocarcinoma group were significantly higher than benign gastric wall group, with $P < 0.0001$, $P = 0.0001$, $P = 0.0445$ and $P < 0.0001$, respectively

Table 2 Comparison of IC and nIC values between gastric cancer and benign lesion groups

Group	Number	ICAP(100 μg/ml)	ICPP(100 μg/ml)	nICAP	nICPP
Benign	108	9.388 (7.497, 12.740)	17.233 (14.448, 18.798)	0.111 (0.076, 0.141)	0.264 (0.068, 0.328)
Cancer	87	12.900 (11.508, 14.832)	20.000 (18.623, 22.000)	0.115 (0.105, 0.141)	0.423 (0.392, 0.453)
Z value		5.870	3.894	2.009	10.137
P value		< 0.0001	=0.0001	=0.0445	< 0.0001

Abbreviations: *ICAP* arterial phase iodine concentration, *ICPP* portal venous phase iodine concentration, *nICAP* normalized arterial phase iodine concentration, *nICPP* normalized portal venous phase iodine concentration

and 0.423 (0.392, 0.453), respectively. Notably, these values were significantly higher in gastric cancer group than those in benign gastric wall lesions group [$Z = 5.870$ (ICAP), 3.894 (ICPP), 2.009 (nICAP) and 10.137 (nICPP); $P < 0.005$].

Comparison of IC and nIC values between gender, age, thickness, location and histological types of gastric adenocarcinoma

As compared to female patients, the values of ICAP, ICPP, nICAP and nICPP were slightly higher in male patients (Table 3). However, none of these differences were statistically significant [$Z = 0.922$ (ICAP), 1.372 (ICPP), 1.636 (nICAP) and 1.449 (nICPP); $P > 0.05$]. All gastric cancer patients were divided into young (≤55 years old) and older (> 55 years old) groups according to the mean age of 55 years old. The values of ICAP, ICPP, nICAP and nICPP in young group were slightly higher than those in older group, but the differences were not statistically significant ($Z = 0.613$, 1.066, 1.935 and 0.583, respectively; $P > 0.05$). In addition, the patients were divided into small (≤3.1 cm) and large (> 3.1 cm) tumor groups according to the mean thickness of 3.1 cm. The values of ICAP, ICPP, nICAP and nICPP in small tumor group were slightly higher than those in large tumor group, but not significantly different ($Z = 1.083$, 0.706, 0.103 and 1.272, respectively; $P > 0.05$). Similarly, the values of ICAP, ICPP, nICAP and nICPP were not significantly different among the three tumor location groups (H values = 0.205, 4.221, 1.859 and 4.836, respectively; $P > 0.05$). Furthermore, the moderately and well-differentiated gastric adenocarcinoma groups were combined into a single group, due to the limited numbers of cases in well-differentiated tumor group ($n = 4$). As shown in Figure 3, the values of ICAP, ICPP, nICAP and nICPP were significantly higher in poorly differentiated group than those in well-differentiated group ($Z = 4.118$, 5.637, 6.729 and 2.950, respectively; $P < 0.05$).

Diagnostic accuracy of IC values in detecting gastric cancer

The AUC values of ICAP, nICAP, ICPP and nICPP for the gastric cancer detection were 0.745, 0.584, 0.662 and 0.923, respectively (Fig. 4 and Table 4). Of note, nICPP demonstrated the greatest ability in discriminating gastric cancer.

Besides, the optimal cut-off values of ICAP, nICAP, ICPP and nICPP were 10.343, 0.089, 14.913 and 0.364, respectively. The sensitivities of ICAP, nICAP, ICPP and nICPP were 95.40, 96.55, 98.85 and 91.95%, respectively; while the specificities were 58.33, 37.04, 43.52 and 87.96%, respectively.

Diagnostic accuracy of IC values in discriminating the histological types of gastric adenocarcinoma

The AUC values of ICAP, nICAP, ICPP, and nICPP in discriminating poorly and well-differentiated gastric adenocarcinoma were 0.756, 0.919, 0.851 and 0.684, respectively (Fig. 4 and Table 4). Of note, nICAP demonstrated the greatest ability in discriminating the histological types of gastric adenocarcinoma, whereas nICPP showed the lowest. The optimal cut-off values of ICAP, nICAP, ICPP and nICPP were 14.460, 0.125, 20.461 and 0.431, respectively. The sensitivities of ICAP, nICAP, ICPP, and nICPP were 53.49, 79.07, 69.77 and 60.47%, respectively; while the specificities were 93.18, 97.73, 90.91 and 79.55%, respectively.

Discussion

Spectral CT extends the capabilities of conventional CT, which uses a rapid kilovoltage switching technique to acquire monochromatic images of tissues, in a similar way to those obtained from a single X-ray source [18–20]. Subsequent elemental decomposition analysis can be performed to obtain iodinated contrast attenuation map, thereby allowing iodine density to be calculated [21, 22]. As a result, this can assist the radiologists to address diagnostic errors. Hence, the present study investigated the role of quantitative spectral CT parameters for the discrimination of gastric cancer and its histological types, and examined their correlations with clinical features. The major findings of this study were as follow: (1) IC values in gastric cancer were higher than benign gastric wall lesions, in which nICPP demonstrated the greatest diagnostic efficacy; (2) IC values in poorly differentiated gastric adenocarcinoma were higher than in well-differentiated caners, in which nICAP showed the highest diagnostic efficacy; and (3) IC values were not significantly different between age, gender, tumor thickness and tumor location.

Li *et al. Cancer Imaging*   (2018) 18:42

Page 6 of 10

Table 3 Comparison of IC and nIC values between gender, age, location, thickness and histological types of gastric adenocarcinoma

| Clinical features	Number of cases	ICAP (100 μg/ml)	ICPP (100 μg/ml)	nICAP	nICPP
Gender					
Male	60	13.018 (11.511, 15,780)	20.464 (18.843, 22.570)	0.125 (0.108, 0.147)	0.431 (0.398, 0.462)
Female	27	12.893 (11.456, 14.385)	19.480 (18.635, 21.485)	0.117 (0.105, 0.136)	0.412 (0.389, 0.443)
Z value		0.922	1.372	1.636	1.449
P value		> 0.05	> 0.05	> 0.05	> 0.05
Age					
Young(≤55 y)	41	13.010 (11.483, 16.675)	20.460 (18.868, 22.570)	0.138 (0.108, 0.153)	0.430 (0.400, 0.455)
Older (> 55 y)	46	13.009 (11.450, 14.440)	19.480 (18.780, 22.000)	0.119 (0.107, 0.136)	0.421 (0.389, 0.463)
Z value		0.613	1.066	1.935	0.583
P value		> 0.05	> 0.05	> 0.05	> 0.05
Sites					
Fundus	29	12.900 (11.543, 16.675)	20.010 (18.742, 22.240)	0.119 (0.106, 0.147)	0.423 (0.394, 0.435)
Body	28	13.672 (11.465, 15.787)	21.835 (19.815, 23.040)	0.140 (0.115, 0.151)	0.642 (0.404. 0.486)
Antrum	27	13.674 (11.930, 15.735)	20.200 (19.253, 22.108)	0.127 (0.111,0.141)	0.430 (0.399, 0.472)
H value		0.205	4.221	1.859	4.836
P value		> 0.05	> 0.05	> 0.05	> 0.05
Thickness					
Small (≤3.1 cm)	38	13.205 (11.890, 15.780)	20.332 (19.022, 22.105)	0.128 (0.109, 0.142)	0.433 (0.393, 0.468)
Large (> 3.1 cm)	49	12.780 (11.111, 14.532)	19.815 (18.783, 22.570)	0.119 (0.107, 0.147)	0.417 (0.396, 0.433)
Z value		1.083	0.706	0.103	1.272
P value		> 0.05	> 0.05	> 0.05	> 0.05
Differentiation					
Poorly	43	14.530 (13.168, 15.670)	21.780 (20.030, 23.348)	0.141 (0.127, 0.155)	0.433 (0.411, 0.472)
Well-differentiated	44	11.880 (11.240, 13.120)	18.855 (17.270, 19.800)	0.106 (0.100, 0.113)	0.410 (0.391, 0.431)
Z value		4.118	5.637	6.729	2.950
P value		< 0.0001	< 0.0001	< 0.0001	=0.0032

Abbreviations: *ICAP* arterial phase iodine concentration, *ICPP* portal venous phase iodine concentration, *nICAP* normalized arterial phase iodine concentration, *nICPP* normalized portal venous phase iodine concentration

Iodine concentration reflects the vessel density and the blood volume in different tissue regions during a contrast-enhanced CT scan. Tang et al. [15] reported a high consistency between spectral CT-measured IC and actual IC, and thus it is a useful parameter to indicate the physiological function. The growth and progression of solid tumors depend upon the formation of new blood vessels, which is different from normal tissues or benign lesions. Several studies have reported that CT imaging is useful for distinguishing small hepatocellular carcinoma from other hepatic lesions [23, 24], small intrahepatic mass-forming cholangiocarcinoma from small liver abscess [25], malignant from benign pulmonary nodules [26], and gastric cancer from benign gastric mucosal lesions [11]. Indeed, the quantitative IC measurement is significantly higher in cancerous lesions compared to benign lesions, and its accuracy is greater than that of conventional CT. In addition, Liu et al. examined the patients with papillary thyroid cancer, and their results suggested that nIC measured during AP and PP are significantly higher in metastatic lymph nodes as compared to benign lesions [27]. Taken together, our results
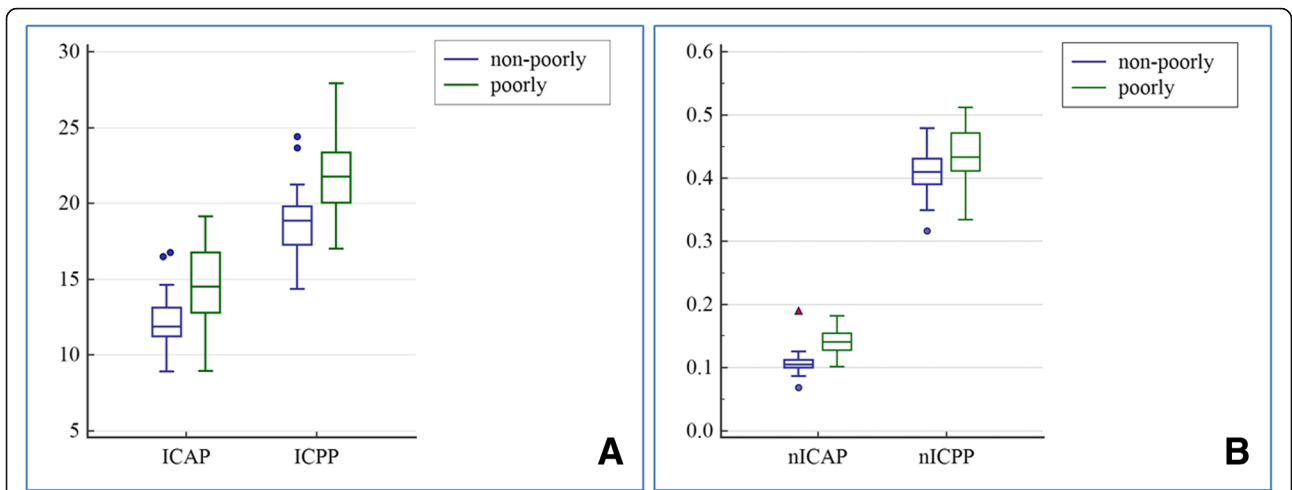
Fig. 3 Differences in IC and nIC values between poorly and well-differentiated gastric adenocarcinoma groups. Box-and-whisker plots (box: 25, 75%; centreline: medium; whisker: min, max) indicate that (**a**) ICAP, ICPP, (**b**) nICAP and nICPP of poorly differentiated gastric adenocarcinoma group were significantly higher than well-differentiated gastric adenocarcinoma group, with $P < 0.0001$, $P < 0.0001$, $P < 0.0001$ and $P = 0.0032$, respectively
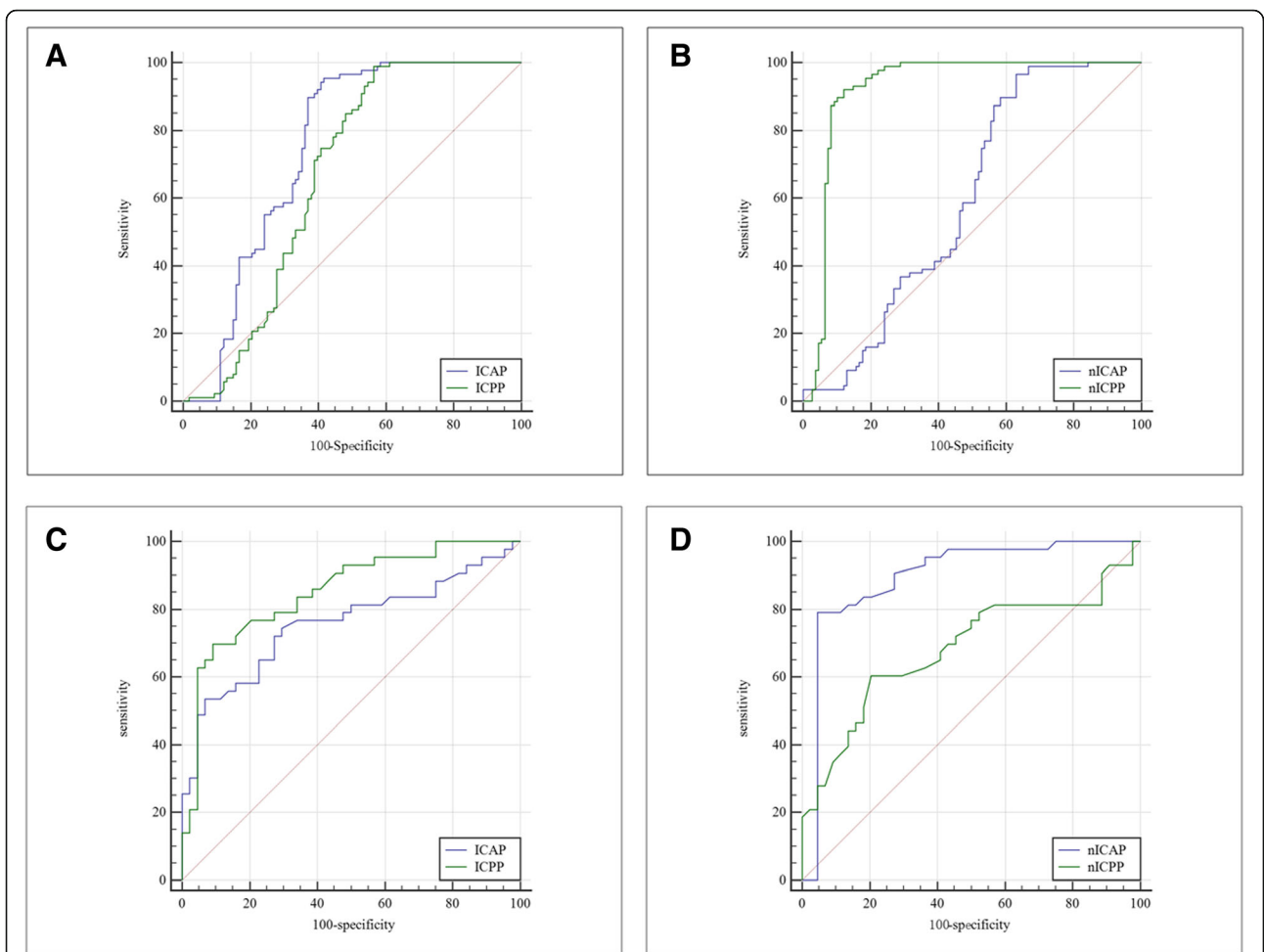
Fig. 4 ROC curves for ICAP, ICPP, nICAP and nICPP. The ROC curves of (**a**) ICAP, ICPP, (**b**) nICAP and nICPP between gastric cancer and benign gastric wall lesions groups. nICPP has the highest AUC value, followed by ICAP, ICPP and nICAP. The ROC curves of (**c**) ICAP, ICPP, (**d**) nICAP and nICPP between poorly and well-differentiated gastric adenocarcinoma groups. nICAP has the highest AUC value, followed by ICPP, ICAP and nICPP

Table 4 The ROC curves of IC and nIC values

ROC	ICAP	ICPP	nICAP	nICPP
Cancer				
AUC	0.745	0.662	0.584	0.923
sensitivity	95.40%	98.85%	96.55%	91.95%
specificity	58.33%	43.52%	37.04%	87.96%
Optimum cutoff values	10.343	14.913	0.089	0.364
Youden index	0.537	0.424	0.336	0.799
Poorly differentiated				
AUC	0.756	0.851	0. 919	0.684
sensitivity	53.49%	69.77%	79.07%	60.47%
specificity	93.18%	90.91%	97.73%	79.55%
Optimum cutoff values	14.460	20.461	0.125	0.431
Youden index	0.467	0.607	0.768	0.400

Abbreviations: *ROC* Receiver operating characteristic curves, *AUC* area under the curve, *ICAP* arterial phase iodine concentration, *ICPP* portal venous phase iodine concentration, *nICAP* normalized arterial phase iodine concentration, *nICPP* normalized portal venous phase iodine concentration

are consistent with the aforementioned studies, in which the values of IC are higher in cancer than in benign lesions, due to the increased angiogenesis during tumor development, leading to their enhancement in CT scan [28].

The degree of tumor differentiation is a predictive and prognosis biomarker for patients with gastric cancer [29], which can be distinguished quantitatively by dual-energy spectral CT (DESCT). Pan et al. [12] evaluated the clinical usefulness of DESCT in the classification and staging of gastric cancer. Their findings indicated that monochromatic images obtained from DESCT can be used to improve the accuracy of preoperative staging, and quantitative IC measurement is helpful in distinguishing the poorly and well-differentiated gastric carcinoma, as well as the metastatic and non-metastatic lymph nodes. A similar pattern of results was obtained, where IC and nIC values were significantly lower in well-differentiated gastric cancer compared to poorly differentiated ones, which can be explained by the differences in tumor angiogenesis. Du et al. [30] have suggested that vascular endothelial growth factor (VEGF) expression and microvessel density (MVD) are closely correlated with histological degree, in which their levels are reduced in early stage gastric carcinoma compared to progressive carcinoma. Chang et al. [31] have reported that MVD is significantly associated with poorly differentiated gastric adenocarcinoma. Moreover, Hu et al. [32] demonstrated that the nIC value of three-phase enhanced CT scan is positively correlated with MVD. Additionally, Chen et al. reported that poorly differentiated gastric cancer exhibited higher MVD and nIC value, and a positive correlation between them [33]. A CT perfusion study on gastric cancer has revealed that the lower the degree of tumor differentiation, the higher the permeability surface area [34]. These findings indicate that poorly differentiated tumors may

increase vasopermeability and immature endothelial cells, thereby explaining the high values of IC and MVD in gastric patients with poorly differentiated adenocarcinoma.

nIC can minimize the effects of individual variability, such as contrast dose, injection rate and individual differences in circulation, and thereby it is more efficacy than IC. Both nICAP and nICPP were found to be significantly different between gastric cancer group and benign gastric wall lesions group, as well as between poorly differentiated group and well-differentiated group. In particular, nICAP demonstrated a higher efficiency in the diagnosis of poorly differentiated gastric adenocarcinoma, with AUC, sensitivity and specificity of 0.896, 79.07 and 95.45%, respectively. Meanwhile, nICPP showed a higher efficacy for the detection of gastric cancer, with AUC, sensitivity and specificity of 0.923, 91.95 and 87.96%, respectively. These results can be partly explained by different functional roles of nICAP and nICPP. nICAP mainly reflects the capillary density and the blood supply of gastric carcinomas, while nICPP may indicate the flow of blood supply and the retention of contrast agent in intrasvasular and extravascular space following AP. It is noticeable that venous phase enhancement is more prominent in gastric cancer, suggesting that PP enhancement characteristics are more useful for the detection of gastric cancer. Besides, the reason why PP is less effective than AP in distinguishing histological types may be due to the influence of blood flow. In addition, nICPP has been reported to exert a high sensitivity in differentiating malignant gastric mucosal lesions from normal gastric mucosa [11]. Furthermore, studies on the diagnostic efficacy of tumor differentiation degree are inconsistent [35, 36], which may be due to the different biological behaviors of tumors and degrees of differentiation. A previous study has found that the values of IC and nIC of poorly differentiated adenocarcinoma are not significantly different compared to those of moderately and well-differentiated adenocarcinomas in AP [17]. These inconsistent results may be attributed to different patient populations and scan protocol. In that study, patients were subjected to triple-phase CT imaging, including AP at 25 s, which are different from ours. In sum, DESCT is more useful in evaluating gastric cancer with a delay AP scan protocol.

Apart from that, Karim et al. [37] reported that younger age is correlated with the histology grade of gastric cancer. However, the histology grade is not correlated with gender and tumor location [38]. In addition, Wang et al. [38] demonstrated that tumour size is a prognostic factor in patients with advanced gastric cancer. In the present study, no significant differences were found in the values of ICAP, ICPP, nICAP and nICPP between age, gender, tumor thickness and tumor location.

There are some unavoidable limitations in this preliminary study. First, DESCT scans were performed on the

Li *et al. Cancer Imaging* (2018) 18:42

Page 9 of 10

first-generation Discovery CT750 HD scanner with a fixed mA value of 600 mA. This yielded a CTDIvol of 23.84 mGy, which is considerably high in current clinical practise settings. With the introduction of the second-generation CT750 HD scanner, the radiation dose has been reduced to 30% in GSI mode, and further dose reduction is forthcoming. Second, this is a retrospective study, and the sample size was relatively small, especially the number of patients with well-differentiated adenocarcinoma was too low to to allow a statistical comparison with moderately and poorly differentiated ones. Third, only patients with gastric adenocarcinoma were enrolled in this study, patients with other histological types of gastric cancer were not taken into account. Moreover, it was difficult to obtain pathologic confirmation of the entire gastric wall in non-cancer patients, and the patients with gastric inflammation and normal gastric wall were grouped together. Finally, since DESCT is a relatively new technique for gastric cancer, it may hinder the adaptation process based on these preliminary results.

Conclusions

In conclusion, this preliminary study compared the quantitative spectral CT parameters between benign lesion and gastric cancer groups, as well as different histological types of gastric adenocarcinoma. IC values can be used to accurately identify gastric cancer and quantitatively assess the degree of differentiation, without being affected by age, gender, tumor thickness and tumor location. These findings may improve the preoperative staging of gastric cancer, and lay the foundations for modern functional imaging in oncology. However, further studies with larger sample sizes are needed to draw a firm conclusion.

Abbreviations
AP: Arterial phase; AUC: Area under the curve; CT: Computed tomography; CTDIvol: CT dose index volume; DEsCT: Dual-energy spectral CT; IC: Iodine concentration; ICC: Intraclass correlation coefficient; MD: Material decomposition; MVD: Microvessel density; nIC: Normalized iodine concentration; PP: Portal venous phase; ROC: Receiver-operating characteristics analysis; ROI: Regions-of-interest; SD: Standard deviation; VEGF: Vascular endothelial growth factor

Availability of data and materials
Please contact author for data requests.

Authors' contributions
RL: manuscript preparation, literature research, data analysis, statistical analysis and manuscript editing; JL: data acquisition and statistical analysis; PL: literature research and data analysis; XP W: data acquisition; JB G: study conception and design, manuscript review and guarantor of integrity of the entire study. All authors read and approved the final manuscript.

Ethics approval and consent to participate
The study protocol was approved by Institutional Review Board of our institution, and written informed consent was obtained from each participant in accordance with the Declaration of Helsinki.

Consent for publication
Not applicable.

Competing interests
The authors declare that they have no competing interests.

Publisher's Note
Springer Nature remains neutral with regard to jurisdictional claims in published maps and institutional affiliations.

Author details
[1]Department of Radiology, the First Affiliated Hospital of Zhengzhou University, No. 1, East Jianshe Road, Zhengzhou 450052, Henan, China. [2]Department of Radiology, the Affiliated Cancer Hospital of Zhengzhou University, Henan Cancer Hospital, No. 127, Dongming Road, Zhengzhou 450008, Henan, China.

References
1. Torre LA, Bray F, Siegel RL, et al. Global cancer statistics, 2012. CA Cancer J Clin. 2015;65:87–108.
2. Dicken BJ, Bigam DL, Cass C, et al. Gastric adenocarcinoma: review and considerations for future directions. Ann Surg. 2005;241:27–39.
3. Wong BC, Lam SK, Wong WM, et al. Helicobacter pylori eradication to prevent gastric cancer in a high-risk region of China: a randomized controlled trial. JAMA. 2004;291:187–94.
4. Yan SY, Hu Y, Fan JG, et al. Clinicopathologic significance of HER-2/neu protein expression and gene amplification in gastric carcinoma. World J Gastroenterol. 2011;17:1501–6.
5. Bang YJ, Kang YK, Kang WK, et al. Phase II study of sunitinib as second-line treatment for advanced gastric cancer. Investig New Drugs. 2011;29:1449–58.
6. Sekiguchi M, Oda I, Taniguchi H, et al. Risk stratification and predictive risk-scoring model for lymph node metastasis in early gastric cancer. J Gastroenterol. 2016;51:961–70.
7. Sasaki T, Koizumi W, Higuchi K, et al. Therapeutic strategy for type 4 gastric cancer from the clinical oncologist standpoint. Gan To Kagaku Ryoho. 2007; 34:988–92.
8. Liu S, Liu Song, Ji C, et al. Application of CT texture analysis in predicting histopathological characteristics of gastric cancers. Eur Radiol. 2017;27:4951–9.
9. Shen Y, Kang HK, Jeong YY, et al. Evalution of early gastric cnncer at multidetector CT with multiplanar reformation and virtual endoscopy. Radiographics. 2011;31:189–99.
10. Lv P, Lin X, Gao J, Chen K. Spectral CT: preliminary studies in the liver cirrhosis. Korean J Radiol. 2012;13:434–42.
11. Meng X, Ni C, ShenY HX, et al. Differentiating malignant from benign gastric mucosal lesions with quantitative analysis in dual energy spectral computed tomography: Initial experience. Medicine (Baltimore). 2017;96:e5878.
12. Pan Z, Pang L, Ding B, et al. Gastric cancer staging with dual energy spectral CT imaging. PLoS One. 2013;8:e53651.
13. Li C, Shi C, Zhang H, et al. Computer-aided diagnosis for preoperative invasion depth of gastric Cancer with dual-energy spectral CT imaging. Acad Radiol. 2015;22:149–57.
14. Li C, Zhang S, Zhang H, et al. Using the K-nearest neighbor algorithm for the classification of lymph node metastasis in gastric cancer. Compu Math Methods Med. 2012;2012:876545.
15. Tang L, Li ZY, Li ZW, et al. Evaluating the response of gastric carcinomas to neoadjuvant chemotherapy using iodine concentration on spectral CT: a comparison with pathological regression. Clin Radiol. 2015;70:1198–204.
16. Li J, Fang M, Wang R, et al. Diagnostic accuracyof dual-energy CT-based nomograms to predict lymph node. Eur Radiol. 2018. https://doi.org/10.1007/s00330-018-5483-2 [Epub ahead of print].
17. Chen LH, Xue YJ, Duan Q. Spectral CT imaging in quantitative evaluation on histological degree of gastric cancers. Chin J Med Imaging Technol. 2013;29: 225–9 Chinese.
18. Hurrell MA, Butler AP, Cook NJ, et al. Spectral Hounsfield units: a new radiological concept. Eur Radiol. 2012;22:1008e13.
19. Tang L, Zhang XP, Sun YS, et al. Spectral CT in the demonstration of the gastrocolic ligament: a comparison study. Surg Radiol Anat. 2013;35:539e45.

20. Li XH, Zhao R, Liu B, et al. Determination of urinary stone composition using dual-energy spectral CT: initial in vitro analysis. Clin Radiol. 2013;68:e370e7.
21. Matsumoto K, Jinzaki M, Tanami Y, et al. Virtual monochromatic spectral imaging with fast kilovoltage switching: improved image quality as compared with that obtained with conventional 120-kVp CT. Radiology. 2011;259:257–62.
22. Silva AC, Morse BG, Hara AK, et al. Dual-energy (spectral) CT: applications in abdominal imaging. Radiographics. 2011;31:1031–46.
23. Lv P, Lin XZ, Li J, et al. Differentiation of small hepatic hemangioma from small hepatocellular carcinoma: recently introduced spectral CT method. Radiology. 2011;259:720–9.
24. Wang Q, Shi G, Qi X, et al. Quantitative analysis of the dual-energy CT virtual spectral curve for focal liver lesions characterization. Eur J Radiol. 2014;83:1759–64.
25. Kim JE, Kim HO, Bae K, et al. Differentiation of small intrahepatic mass-forming cholangiocarcinoma from small liver abscess by dual source dual-energy CT quantitative parameters. Eur J Radiol. 2017;92:145–52.
26. Zhang Y, Cheng J, Hua X, et al. Can spectral CT imaging improve the differentiation between malignant and benign solitary pulmonary nodules? PLoS One. 2016;11:e 0147537.
27. Liu X, Ouyang D, Li H, et al. Papillary thyroid cancer: dual-energy spectral CT quantitative parameters for preoperative diagnosisof metastasis to the cervical lymph nodes. Radiology. 2015;275:167–76.
28. Miles KA. Tumour angiogenesis and its relation to contrast enhancement on computed tomography: a review. Eur J Radiol. 1999;30:198–205.
29. Haist T, Pritzer H, Pauthner M, et al. Prognostic risk factors of early gastric cancer-a western experience. Langenbeck's Arch Surg. 2016;401:667–76.
30. Du JR, Jiang Y, Zhang YM, et al. Vascular endothelial growth factor and microvascular density in esophageal and gastric carcinomas. World J Gastroenterol. 2003;9:1604–6.
31. Chang Y, Niu W, Lian PL, et al. Endocan-expressing microvessel density as a prognostic factor for survival in human gastric cancer. World J Gastroenterol. 2016;22:5422–9.
32. Hu S, Huang W, Chen Y, et al. Spectral CT evaluation of interstitial brachytherapy in pancreatic carcinoma xenografts: preliminary animal experience. Eur Radiol. 2014;24:2167–73.
33. Chen XH, Ren K, Liang P, et al. Spectral computed tomography in advanced gastric cancer: can iodine concentration non-invasively assess angiogenesis? World J Gastroenterol. 2017;23:1666–75.
34. Lee DH, Kim SH, Joo I, et al. CT perfusion evaluation of gastric cancer: correlation with histologic type. Eur Radiol. 2018;28:487–95.
35. Lin LY, Zhang Y, Suo ST, et al. Correlation between dual-energy spectral CT imaging parameters and pathological grades of non-small cell lung cancer. Clin Radiol. 2018;73:412.e1–7.
36. Chuang-Bo Y, Tai-Ping H, Hai-Feng D, et al. Quantitative assessment of the degree of differentiation in colon cancer with dual-energy spectral CT. Abdom Radiol (NY). 2017;42:2591–6.
37. Karim S. Clinicopathological and p53 gene alteration comparison between young and older patients with gastric cancer. Asian Pac J Cancer Prev. 2014; 15:1375–9.
38. Wang HM, Huang CM, Zheng CH, et al. Tumor size as a prognostic factor in patients with advancer gastric cancer in the lower third of the stomach. World J Gastroenterol. 2012;18:5470–5.